PNAS
www.pnas.org

Supplementary Information for

βII-spectrin promotes mouse brain connectivity through stabilizing axonal plasma membranes and enabling axonal organelle transport

Damaris N. Lorenzo, Alexandra Badea, Ruobo Zhou, Peter J. Mohler, Xiaowei Zhuang, Vann Bennett

Damaris N. Lorenzo and Vann Bennett
Email: damaris_lorenzo@med.unc.edu and benne012@mc.duke.edu

This PDF file includes:

www.pnas.org/cgi/doi/10.1073/pnas.1820649116

Materials and Methods

Mouse lines and animal care

Experiments were performed in accordance with the guidelines for animal care of the Institutional Animal Care and Use Committee at Duke University and UNC Chapel Hill. To generate brain-specific βII-spectrin KO mice (*βII-Spec*$^{flox/flox}$/Nestin-Cre, βIISp-KO), *βII-Spec*$^{flox/flox}$ mice, a gift from Dr. Matthew Rasband (27), were crossed with the Nestin-Cre mouse line [B6.Cg-Tg(Nes-cre)1Kln/J, stock number 003771; The Jackson Laboratory]. *βII-Spec*$^{flox/flox}$ animals negative for the Cre transgene were used as littermate controls in all experiments. Mice homozygous for the floxed alleles of βII-spectrin and AnkB (*ßIISp*$^{flox/flox}$*/AnkB*$^{flox/flox}$) were generated by crossing *βII-Spec*$^{flox/flox}$ and *AnkB*$^{flox/flox}$ (51) animals for multiple generations. *ßIISp*$^{flox/flox}$*/AnkB*$^{flox/flox}$ mice were also crossed to the Nestin-Cre line. All mice were housed at 22°C ± 2°C on a 12-hour-light/12-hour-dark cycle and fed ad libitum regular chow and water.

Plasmids

Plasmid used in transfection experiments included: pSynaptophysin-YFP (gift from Dr. Ann Marie Craig), pTGN38-GFP and pTfR-YFP (gifts from Dr. Antonius M. J. VanDongen), pEB3-tdTomato (Addgene plasmid #50708, gift from Dr. Erik Dent), and pLAMP1-GFP (Addgene plasmid # 16290, gift from Ron Vale). To generate pmScarlet-WT-βII-spectrin, pmScarlet-K2207Q-βII-spectrin, and pmScarlet-Y1874A-βII-spectrin, the coding sequence of human βII-spectrin were amplified by PCR as AgeI/HindIII fragments respectively from peGFP-C3- WT-βII-spectrin, peGFP-C3-K2207Q-βII-spectrin, and peGFP-C3-Y1874A-βII-spectrin vectors (52), and cloned into the corresponding sites of pmScarlet-C1 (Addgene plasmid # 85042, gift from Dorus Gadella). pCAG-BFP or pCAG-Cre-BFP plasmids were previously reported (53). All plasmids were verified by full-length sequencing prior to transfection.

Antibodies

Affinity-purified rabbit antibodies against βII-spectrin, βIV-spectrin, ankyrin-B (AnkB), and ankyrin-G (AnkG), used at a 1:500 dilution for immunohistochemistry and 1:5000 for western blot, were generated in our laboratories and have been previously described (14, 53). Other antibodies included mouse anti-synaptophysin (1:1000, #S5768, Sigma), mouse anti-αII-spectrin D8B7 clone (1:1000, # 803201, BioLegend), goat anti-βIII-spectrin N-19 clone (1:300, #sc-9660, Santa Cruz Biotechnology), rabbit anti-ANK1 (ankyrin-R, AnkR) (1:1000, # ARP42566_T100, Aviva Systems), mouse anti-α-tubulin clone 1E4C11 (1:5000, #66031-1-Ig, Proteintech), rat anti-MBP (1:1000, #aa82-87, Bio-Rad), mouse anti-neurofilament clone SMI 311(1:500, # 837802, BioLegend), and chicken anti-MAP2 (1:1000, # ab5392, Abcam). We also used use mouse anti-p150Glued (1:1000, # 610473, BD Biosciences), mouse anti-DIC (1:1000, #MAB1618, EMD Millipore), mouse anti-KIF5B (1:1000, #MAB1613, EMD Millipore), rabbit anti-KIF3A (1:1000, #ab11259, Abcam), mouse anti-KIF1A (1:1000, # 612094, BD Biosciences), rabbit anti-α-tubulin (1:1000, #11224-1-AP, Proteintech), and mouse anti-GAPDH (1:1000, # 60004-1-Ig, Proteintech).

For adducin labeling of axons in STORM labeling of axons in STORM images we used rabbit anti-α-adducin (1:200, #ab51130, Abcam). Secondary antibodies purchased from Life Technologies were used at 1:400 dilution for fluorescence-based detection by confocal microscopy and STORM, and included donkey anti-rabbit IgG conjugated to Alexa Fluor 568 (#A10042), donkey anti-mouse IgG conjugated to Alexa Fluor 488 (#A21202), goat anti-chicken conjugated to Alexa Fluor 647 (#A21469), and donkey anti-rabbit IgG conjugated to Alexa Fluor 647 (#A31573). Fluorescent signals in western blot analysis were detected using goat anti-rabbit 800CW (1:15000, #926-32211, LiCOR), goat anti-mouse 680RD (1:15000, #926-68070, LiCOR), and goat anti-rat 800CW (1:15000, #925-32219, LiCOR).

Neuronal culture

Primary hippocampal and cortical neuronal cultures were established from E15.5 mice. Hippocampi or cortices were dissected in Hibernate E (Life Technologies) and digested with

0.25% trypsin in HBSS (Life Technologies) for 15 min at 37°C. Tissue was washed three times with HBSS and dissociated in DMEM (Life Technologies) supplemented with 5% fetal bovine serum (FBS, Genesee), B27 supplement (Life Technologies), 2 mM Glutamax (Life Technologies), and penicillin/streptomycin (Life Technologies), and gently triturated through a glass pipette with a fire-polished tip. Dissociated cells were filtered through a 70 μm cell strainer to remove any residual non-dissociated tissue and plated onto poly-D-lysine- and laminin-coated dishes (MatTek) for transfection and time-lapse microscopy imaging. For STORM imaging neurons were plated onto poly-L-lysine- and laminin-coated 12-mm coverslips (BD bioscience). For all cultures, media was replaced 16 hours after plating with serum-free Neurobasal-A medium containing B27 and Glutamax (culture medium). 5 μM cytosine-D-arabinofuranoside (Sigma) was added to the culture medium to inhibit the growth of glial cells three days after plating. Neurons were fed twice a week with freshly made culture medium until use.

Neuronal Transfection

For time-lapse imaging experiments DIV0-DIV5 hippocampal neurons were transfected with 1μg of each plasmid DNA following a modified Ca^{2+}-phosphate transfection protocol (54) using the CalPhos Mammalian Transfection Kit (Clontech) and imaged 48-96 hours after transfection. For experiments that evaluate axonal length, DIV0 control neurons were transfected with 500 ng of pmScarlet-C1. βII-SpKO neurons were transfected with either pmScarlet-C1 or with 1 μg of pmScarlet-βII-spectrin rescue plasmids using a similar Ca^{2+}-phosphate transfection protocol. Neurons were processed for immunofluorescence 3-7 days after transfection. For experiments that evaluate transport dynamics after dual knockdown of AnkB and βII-spectrin, *AnkB*$^{flox/flox}$*/βII-Spec*$^{flox/flox}$ neurons were also transfected using the Ca^{2+}-phosphate method. In this case, DIV0 neurons were transfected with 1μg of either pCAG-BFP or pCAG-Cre-BFP plasmids in combination with 1μg of each of the other plasmids and imaged at DIV7.

Histology and immunohistochemistry

Brains from mice two-weeks and older were fixed by transcardial perfusion with phosphate-buffered saline (PBS) and 4% paraformaldehyde (PFA) followed by overnight immersion in the same fixative. Brains from PND0-PND14 mice were fixed by direct immersion in 4% PFA for 36 hours. After fixation, brains were rinsed with PBS, transferred to 70% ethanol for at least 24 hours, and paraffin-embedded. 7-μm coronal brain sections were cut using a Leica RM2155 microtome and mounted on glass slides. Sections were analyzed by hematoxylin and eosin (H&E) staining or immunostaining. For antibody staining, sections were deparaffinized and rehydrated using a standard protocol of washes: 3 × 3-min Xylene washes, 3 × 2-min 100% ethanol washes, and 1 × 2-min 95%, 80%, and 70% ethanol (each) followed by at least 5 min in PBS. Sections were then processed for antigen retrieval using 10 mM sodium citrate, pH 6 in the microwave for 20 min. Sections were allowed to cool, washed in PBS, and blocked using antibody buffer (2% bovine serum albumin (BSA), 1% fish oil gelatin, 5% donkey serum, and 0.02% Tween 20 in PBS) for 1 hour at room temperature. Tissue sections were then subsequently incubated overnight with primary antibodies at 4°C and with secondary antisera for 1.5 hours at 4°C, washed with PBS, and mounted with Prolong Gold Antifade reagent (Life Technologies).

Neuronal cultures were washed with cold PBS, fixed with 4% PFA for 15 min, and permeabilized with 0.2% Triton-X100 in PBS for 10 min at room temperature. Neurons were blocked in antibody buffer for 1 hour at room temperature and processed for fluorescent staining as tissue sections. For STORM imaging DIV10 cultured neurons were initially fixed and extracted for 1 min in a solution of 0.3% (v/v) glutaraldehyde and 0.25% (v/v) Triton X-100 in cytoskeleton buffer (CB) (10 mM MES, pH 6.1, 150 mM NaCl, 5 mM EGTA, 5 mM glucose, and 5 mM $MgCl_2$). Samples were post-fixed for 15 min in 2% (v/v) glutaraldehyde in CB and treated with freshly prepared 0.1% (w/v) sodium borohydride for 7 min to reduce background fluorescence caused by glutaraldehyde fixation.

Immunoblots

Protein homogenates from mouse brains were prepared in 1:9 (wt/vol) ratio of homogenization buffer (8M urea, 5% SDS (wt/vol), 50mM Tris pH 7.4, 5mM EDTA, 5mM N-ethylmeimide, protease and phosphatase inhibitors) and heated at 65ºC for 15 min to produce a clear homogenate. Total protein lysates were mixed at a 1:1 ratio with 5x PAGE buffer (5% SDS (wt/vol), 25% sucrose (wt/vol), 50mM Tris pH 8, 5mM EDTA, bromophenol blue) and heated for 15 min at 65ºC. Samples were resolved by SDS-PAGE on 3.5-17.5% acrylamide gradient gels in Fairbanks Running Buffer (40mM Tris pH 7.4, 20mM NaAc, 2mM EDTA, 0.2%SDS (wt/vol)). Proteins were transferred overnight onto 0.45 µm nitrocellulose membranes (#1620115, BioRad) at 4°C. Transfer efficiency was determined by Ponceau-S stain. Membranes were blocked in TBS containing 5% non-fat milk for 1 hour at room temperature and incubated overnight with primary antibodies diluted in antibody buffer (TBS, 5% BSA, 0.1% Tween-20). After 3 washes in TBST (TBS, 0.1% Tween-20), membranes were incubated with secondary antibodies diluted in antibody buffer for two hours at room temperature. Membranes were washed 3x for 10 minutes with TBST and 2x for 5 minutes in TBS. Protein-antibody complexes were detected using the Odyssey® CLx Imaging system (LI-COR).

Immunoprecipitation

For immunoprecipitation experiments, total protein homogenates from brains were prepared in PBS containing 150 mM NaCl, 0.32 M sucrose, 2 mM EDTA, 0.1% Triton X-100, 0.1% sodium deoxycholate, 0.1% SDS, and protease inhibitors (10 µg/ml AEBSF, 30 µg/ml benzamidine, 10 µg/ml pepstatin, and 10 µg/ml leupeptin). Cell lysates were incubated with rotation for 1 hour at 4°C and centrifuged at 100,000 x g for 30 min. Soluble fractions were collected and precleared by incubation with Protein-G magnetic beads (#1614023, Bio-Rad) for 1 hour in the cold. Samples were subjected to immunoprecipitation in the presence of protein-G magnetic beads/antibody or protein-G magnetic beads/isotype control complexes overnight at 4°C. Immunoprecipitation samples were resolved by SDS-PAGE and Western blot and signal detected using the Odyssey® CLx imaging system.

Membrane fractionation essay

Membrane isolation from brain homogenates was conducted as previously reported (55). In brief, four brains from PND1 control or βII-SpKO mice were homogenized in TMEE buffer (50 mM Tris, pH 7.4, 5 mM MgSO4, 1 mM EGTA, 0.5 mM EDTA, and protease inhibitors). Nuclei were pelleted by centrifugation at 1600 rpm for 10 min at 4°C. The postnuclear supernatant (PNS) was fractionated by centrifugation at 44,700 rpm for 30 min at 4°C (SW55Ti rotor) into supernatant (soluble fraction) and pellet (total membrane fraction). The pellet was then brought to 2 M sucrose in TMEE (1:4 vol/vol) and overlaid stepwise with 1.2 M and 0.2 M sucrose in TMEE. The gradient was centrifuged at 44,700 rpm for 60 min at 4°C (SW55Ti rotor) and floated membranes were collected from the 1.2 M/0.2 M sucrose interface. Membranes were diluted to 700 µl in TMEE and re-pelleted at 44,700 rpm for 30 min at 4°C. The final pellet was dissolved in 5xPAGE and proteins in each fraction were solved by SDS-PAGE and Western Blot.

STORM imaging

For actin imaging, DIV 14 neurons were fixed using 2% glutaraldehyde after an extraction step as previously described (4), and DIV 20 neurons were fixed using 4% paraformaldehyde (PFA) as previously described (7). For adducin imaging, both DIV 14 neurons and DIV 20 neurons were fixed using 4% PFA. Actin and adducin were labeled using Alexa Fluor 647 conjugated phalloidin and anti-α-adducin antibody, respectively, following a previously described protocol (7). STORM imaging was conducted in PBS containing 100 mM cysteamine, 5% glucose, 0.8 mg/mL glucose oxidase (Sigma-Aldrich), and 40 µg/mL catalase (Roche Applied Science). The STORM setup was based on a Nikon Eclipse Ti-U inverted optical microscope as previously reported (4). For 3D STORM imaging, a cylindrical lens was inserted into the imaging path so that images of single molecules were elongated in x and y for molecules on the proximal and distal sides of the focal plane (relative to the objective), respectively.

Continuous illumination of 647-nm laser (~2kW/cm^2) was used to excite fluorescence from Alexa647 molecules and switch them into the dark state. Continuous illumination of the 405-nm laser was used to reactivate the fluorophores to the emitting state. The power of the activation lasers (typical range 0-1 W/cm^2) was adjusted during image acquisition so that at any given instant, only a small and optically resolvable fraction of the fluorophores in the sample was in the emitting state. A typical STORM image was generated from a sequence of about 30,000 image frames at a frame rate of 60 Hz. The recorded STORM movies were analyzed according to previously described methods (56). Super-resolution images were reconstructed from the molecular coordinates by depicting each location as a 2D Gaussian peak. Localization precisions were ~10 nm for lateral (xy) and ~22 nm for axial (z) directions measured in SD, or ~25 nm for lateral and ~50 nm for axial directions measured in FWHM. 1D autocorrelation analysis was performed and the average autocorrelation amplitudes were calculated as previously described (7).

Fluorescence image acquisition and image analysis

Confocal microscope images were taken using a Zeiss LSM780 using 405-, 488-, 561-, and 633-nm lasers. Single images and Z-stacks with optical sections of 1 µm intervals and tile scans were collected using the ×10 (0.4 NA) and ×40 oil (1.3 NA) objective lens. Images were processed, and measurements taken and analyzed, using Zeiss Zen, Volocity (Perkin Elmer), or NIH ImageJ software. Three-dimensional rendering of confocal Z-stacks was performed using Volocity with the 3D rendering option set to opacity.

Time-lapse video microscopy and movie analyses

Live microscopy of neuronal cultures was carried out using a Zeiss 780 laser scanning confocal microscope (Zeiss) equipped with a GaAsP detector and a temperature- and CO_2-controlled incubation chamber. Movies were taken in the mid-axon around 60 µm away from the soma and captured at a rate of 1 frame/second for time intervals ranging from 60-300 seconds with a 40x oil objective (1.4NA) using the zoom and definite focus functions. Movies of EB3-tdT were captured in the distal portion of the axon. Time-lapse images were exported as 15 frames/sec video files using the Zen Black acquisition and imaging software (Zen Black, Zeiss) and were processed and analyzed using ImageJ (http://rsb.info.nih.gov/ij). Kymographs were obtained using the KymoToolBox plugin for ImageJ (57) (https://github.com/fabricecordelieres/IJ_KymoToolBox). In details, space (x axis in µm) and time (y axis in sec) calibrated kymographs were generated from video files. In addition, the KymoToolBox plugin was used to manually follow a subset of particles from each kymograph and report the tracked particles on the original kymograph and video files using a color code for movement directionality (red for anterograde, green for retrograde and blue for stationary particles). Quantitative analyses were performed manually by following the trajectories of individual particles to calculate dynamic parameters including, net and directional velocities and net and directional run length, as well as time of pause or movement in a direction of transport. Anterograde and retrograde motile vesicles were defined as particles showing a net displacement >3 µm in one direction. Stationary vesicles were defined as particles with a net displacement <2 µm.

Electron microscopy

Control and βII-SpKO mice were perfused at PND25 with 2% PFA and 2.5% glutaraldehyde in 0.1 M sodium cacodylate buffer (pH 7.4) at room temperature. Brain were post-fixed in the same buffer at 4°C for 5 additional days. Fixed brains were sectioned using a microslicer to generate ~2mm-thick coronal sections. Matching corpus callosum areas from control and βII-SpKO were further dissected, fixed overnight, sliced and processed by the Microscopy Service Laboratory at UNC-Chapel Hill. TEM images were acquired with a JEOL 1230 transmission electron microscope. The g-ratio of myelinated corpus callosum axons was calculated using the g-ratio plugin for ImageJ (http://gratio.efil.de/).

Magnetic resonance histology and Diffusion Tensor Image analysis

Brain specimens from PND21 control (n=6) and littermate βII-SpKO (n=7) mice were actively stained by transcardial perfusion with 0.9% saline at a rate of 8 ml/min for 5 min. Fixation was performed with a 10% solution of neutral phosphate-buffered formalin containing 10% (50 mM) of the contrast agent Gadoteridol (ProHance) at the same rate for 5 min. The fixed specimens were transferred to a 0.01 M solution of PBS containing 0.5% (2.5 mM) Gadoteridol at 4 °C for 5-7 days to rehydrate the tissue. Brains were kept in the skull for the entire procedure, including during the magnetic resonance scanning to avoid physical distortion, and were immersed in perfluoropolyether (Galden Pro) for susceptibility matching.
MRI was performed using a 9.4T, 8.9 cm vertical bore Oxford magnet, with shielded coils, providing gradients up to 2000 mT/m (Resonance Research, Inc.), controlled by an Agilent Direct Drive Console (Agilent Technologies), and custom-made solenoid coils. Imaging protocols relied on 3D spin echo diffusion weighted acquisition, with diffusion sensitization directions, interspersed with 3 non-diffusion weighted cans. To accelerate acquisition, we used compressed sensing with a compression factor of 4. The imaging matrix was 368x184x184 mm; field of view 22x11x11 mm, repetition time TR=90ms; echo time TE=12 ms; diffusion amplitude = 130.67 G/cm, durations were 4ms, separation was 6 ms, b=4000 s/mm2; BW=125kHz. Images were reconstructed at 55 μm isotropic resolution. Total imaging scan time per animal was 7 h and 11 min.
Image Analysis was performed using a high-performance computing (HPC) pipelines for image reconstruction relying on the Berkeley Advanced Reconstruction Toolbox (58, 59), for image segmentation (60), and for computing regional and voxel-wise statistics using a symmetric brain atlas with 332 regions (https://arxiv.org/pdf/1709.10483) as refined based on definitions previously used (31). Diffusion tensor estimation and tractography based connectomes were calculated using DSIStudio (dsi-studio.labsolver.org/) (60). 200,000 seeds were randomly placed in the mask brain. Fractional anisotropy threshold was set at 0.3 and the angular threshold was 65°. The whole brain analysis is based on tracks generated from seeds placed over all the brain.

Statistical analysis

GraphPad Prism (GraphPad Software) was used for statistical analysis. Two groups of measurements were compared by unpaired, two-tailed Student's t test. Multiple groups were compared by one-way ANOVA followed by a Dunnett's multiple comparisons test. Survival curves were compared using a Mantel-Cox test.

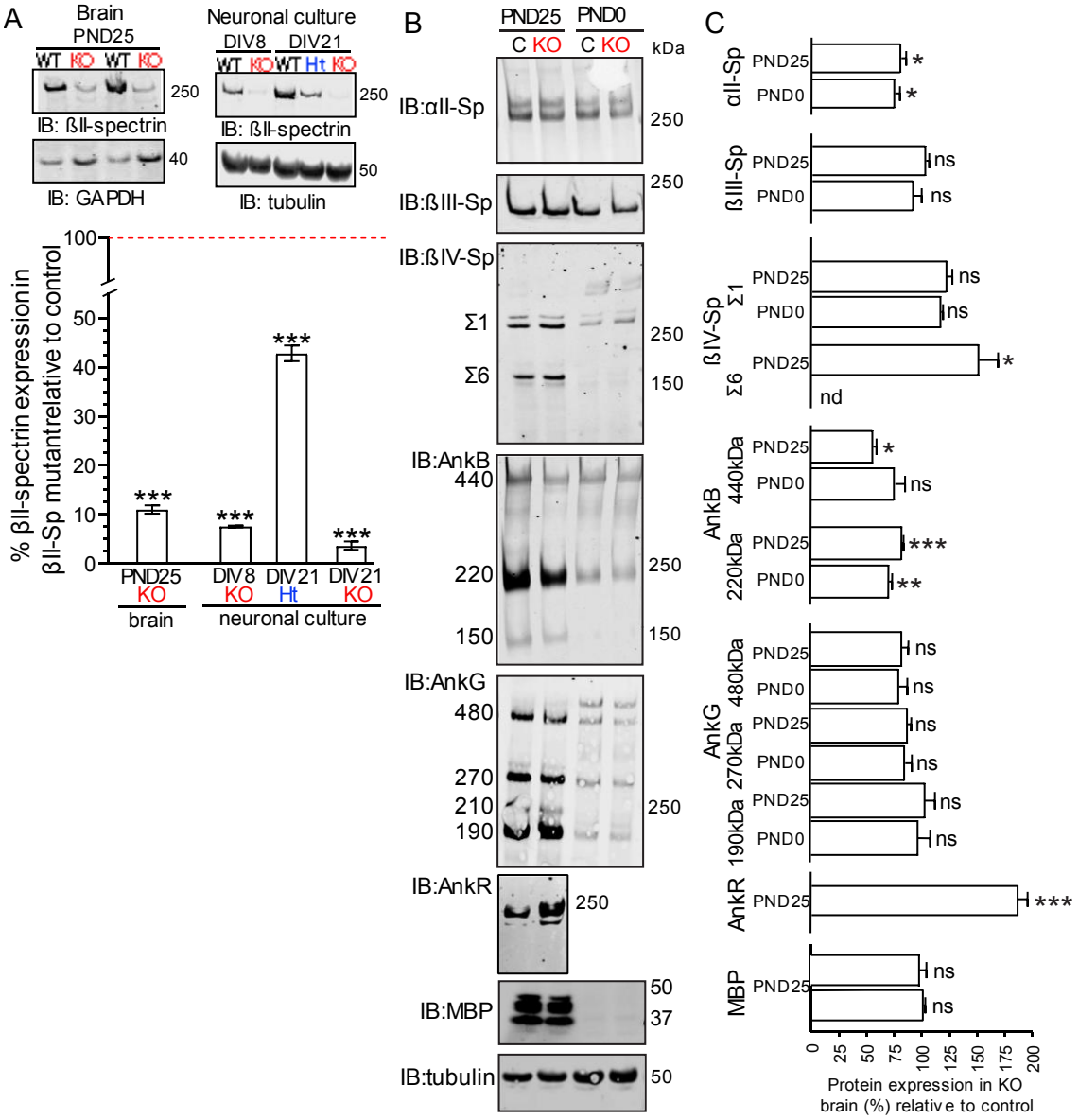

Fig. S1. Loss of βII-spectrin causes changes in the expression levels of cytoskeletal proteins

(A) Immunoblots from total brain lysates from control *ßIISp*$^{flox/flox}$/+ ("WT") and *ßIISp*$^{flox/flox}$/Nestin-Cre ("KO") mice at PND25, and from cortical neuronal cultures from WT, βII-spectrin KO or heterozygous (Ht) embryos at DIV8 and DIV21 using antibodies specific for βII-spectrin. GAPDH and tubulin are loading controls. (B) Western blot analysis of brain homogenates from PND0 and PND25 control (C) and ßII-SpKO mice immunoblotted with antibodies specific for αII-spectrin, βIII-spectrin, βIV-spectrin, AnkB, AnkG, AnkR, and myelin basic protein **(**MBP). Tubulin was used as a loading control. (C) Analysis of protein expression in ßII-SpKO brains relative to control brains for each indicated protein and their isoforms (n=3 brains). Data represent mean ± SEM. Student's t test, ****$p < 0.0001$, ***$p < 0.001$, **$p < 0.01$, *$p < 0.05$, $^{ns}p > 0.05$.

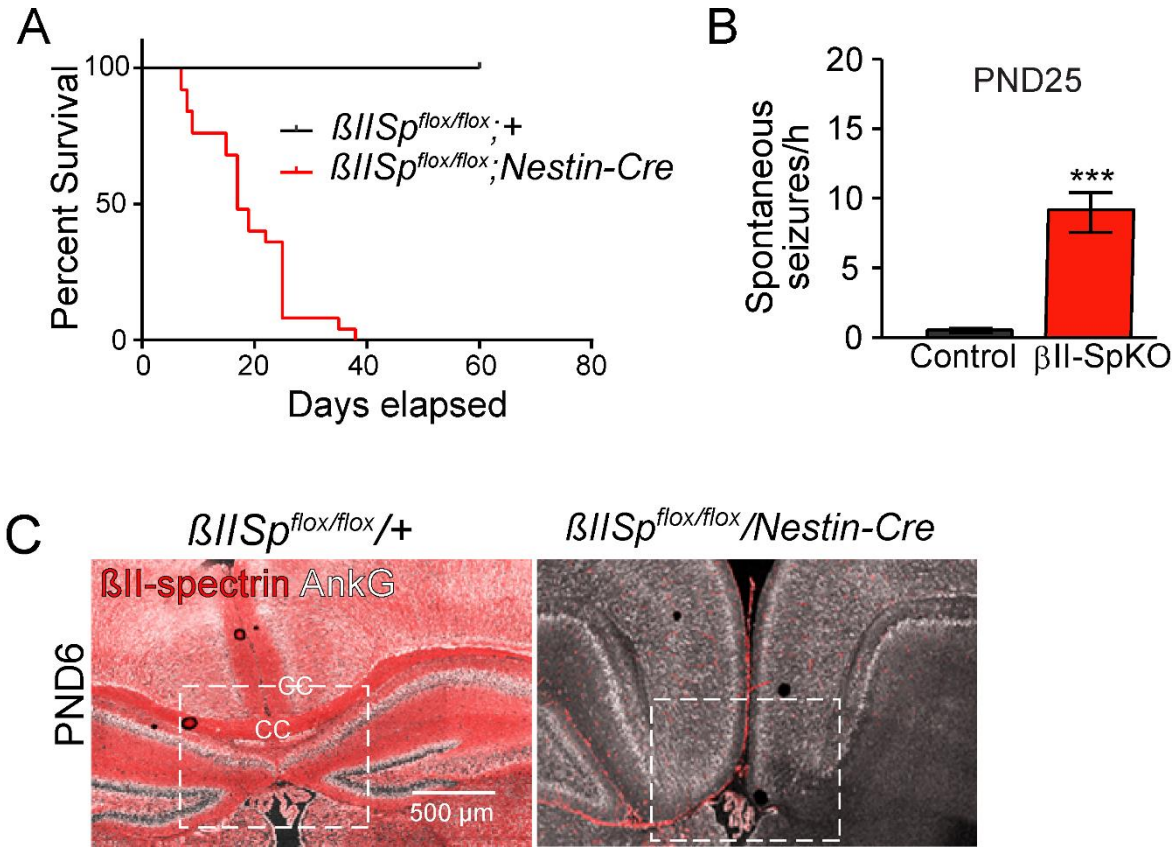

Fig. S2. Loss of brain βII-spectrin causes early postnatal, spontaneous seizures, and loss of the corpus callosum.

(A) Survival curve from *ßIISp*$^{flox/flox}$/+ and *ßIISp*$^{flox/flox}$/Nestin-Cre mice. Mantel-Cox test was used to compare survival. (B) Number of observed spontaneous seizures/hour in *ßIISp*$^{flox/flox}$ and *ßIISp*$^{flox/flox}$/Nestin-Cre PND25 mice (n=12). (C) Images through the CC from *ßIISp*$^{flox/flox}$/+ and *ßIISp*$^{flox/flox}$/Nestin-Cre PND6 brains stained for βII-spectrin and AnkG. White box demarks the CC region. Scale bar, 500 µm. Data represent mean ± SEM. Student's t test, ****$p < 0.0001$, ***$p < 0.001$, **$p < 0.01$, *$p < 0.05$.

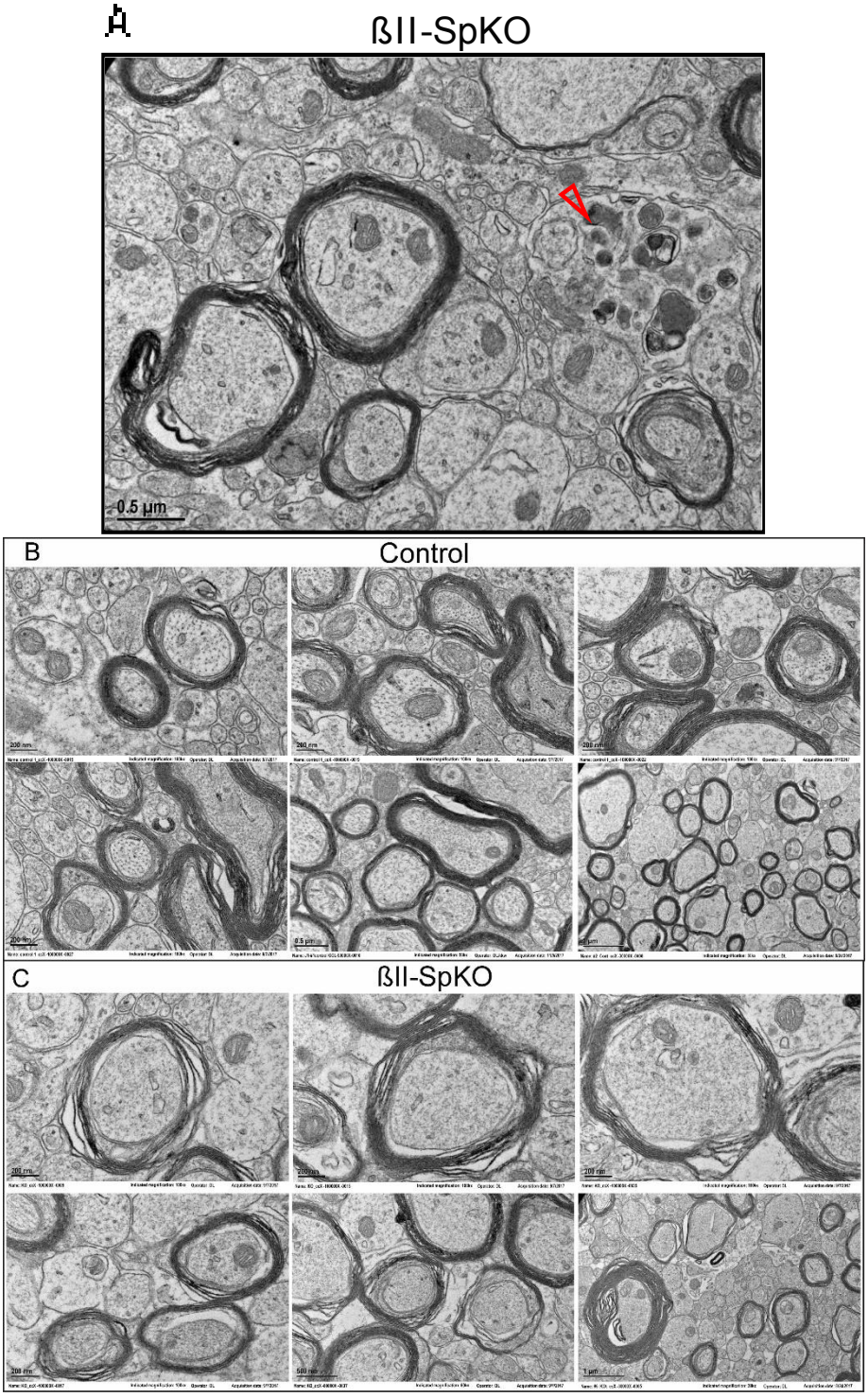

Fig. S3. Loss of βII-spectrin induces axon degeneration.

(A-C) Representative TEM images of brain cross sections through the CC from *ßIISp*$^{flox/flox}$/Nestin-Cre (ßII-SpKO) (A, C) and control (B) PND25 mice (n=3 mice). Red arrowhead indicates the presence of inflammatory microglia. Scale bars, 0.5 µm (A), 200 nm (B and C top row, and bottom row left corner), 500 nm (B and C bottom row middle), and 1 µm (B and C bottom row right corner).

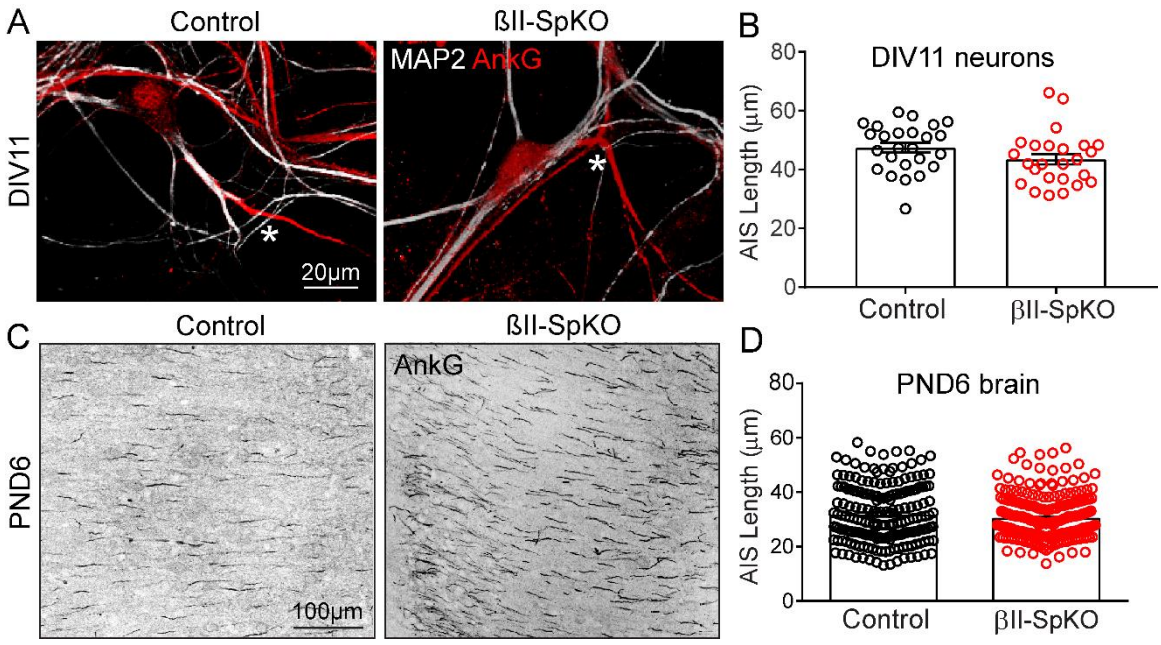

Fig. S4. Loss of βII-spectrin in cultured neurons and mouse brains does not affect AIS length.

(A) Images of DIV11 control and ßII-SpKO neurons stained with antibodies specific for MAP2 (to identify dendrites) and AnkG (to label the AIS, asterisk). Scale bar, 20 µm. (B) Quantification of AIS length in DIV11 neurons (n=25 neurons per genotype). (C) Histological sections through the cortex of PND6 control and ßII-SpKO brains stained for AnkG. Scale bar, 100 µm. (D) Quantification of AIS length from brain sections from control (n=194 neurons) and ßII-SpKO (n=253 neurons) mice. Data represent mean ± SEM. Student's t test.

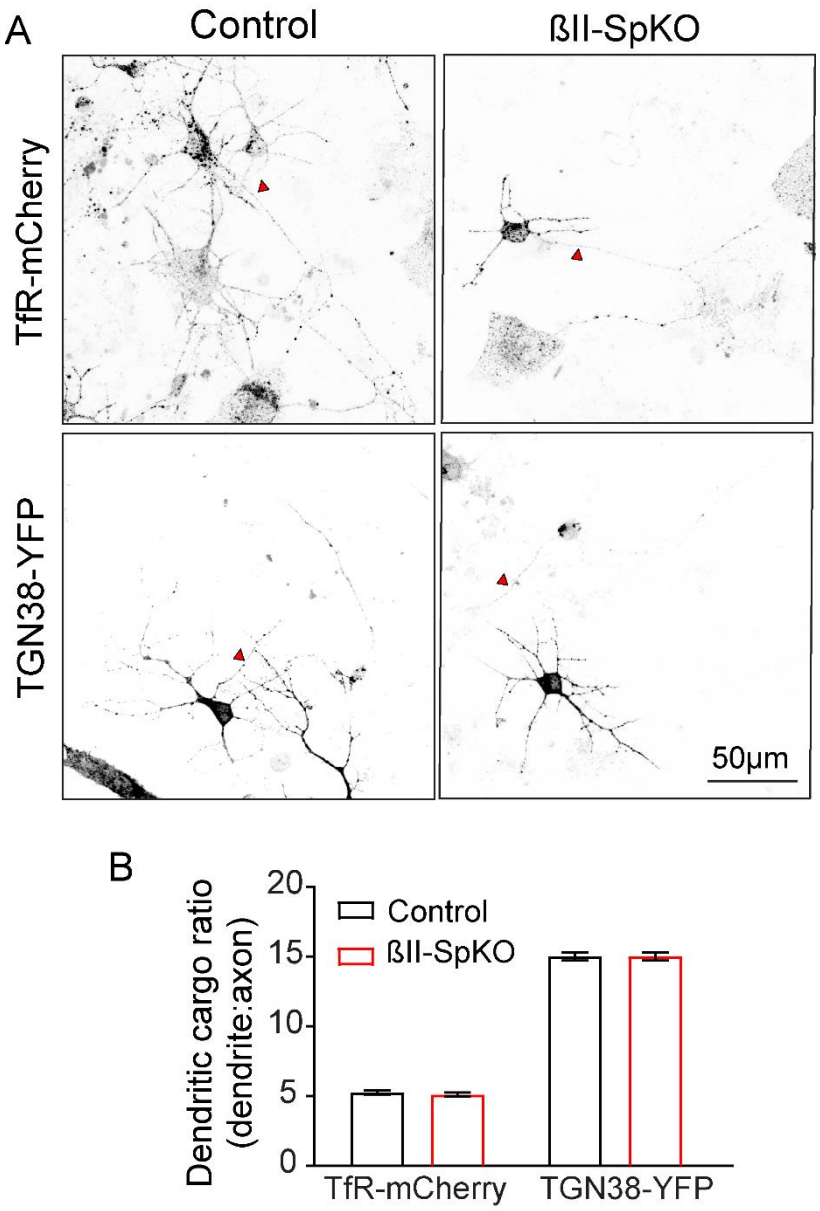

Fig. S5. Loss of neuronal βII-spectrin does not affect the polarized distribution of dendritic cargos

(A) Images of DIV11 control and ßII-SpKO neurons expressing TfR-mCherry or TGN38-YFP. Scale bar, 50 µm. Red arrowheads indicate axons. (B) Quantification of the dendritic to axonal ratio for TfR-mCherry or TGN38-YFP distribution in control (n=10) and ßII-SpKO (n=10) neurons. Data represent mean ± SEM. Student's t test.

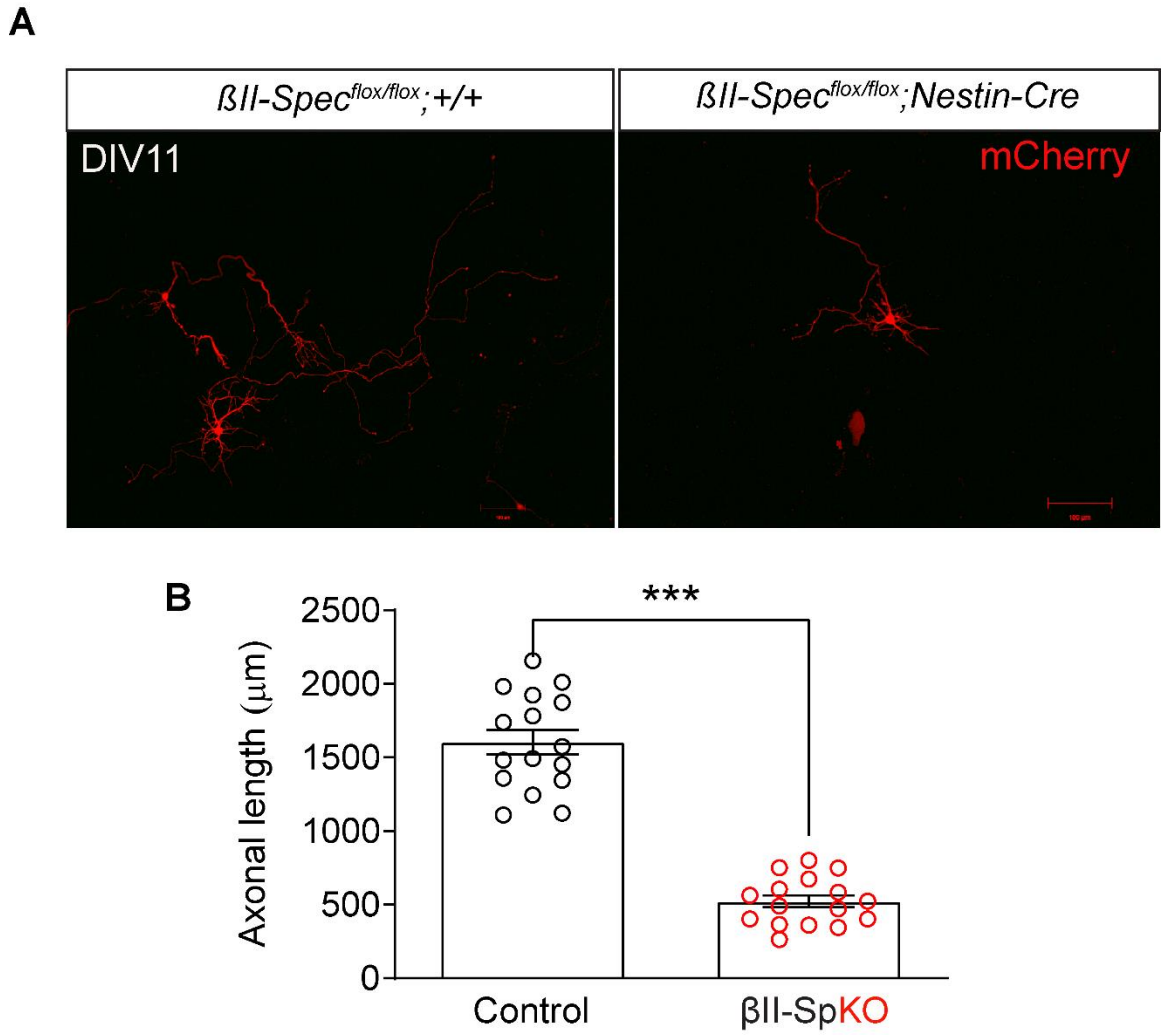

Fig. S6. βII-spectrin is required for axonal elongation of cultured hippocampal neurons

(A) DIV11 control or ßII-SpKO hippocampal neurons transfected at DIV0 with pmCherry. (B) Axonal length in control (n=16), ßII-SpKO (n=16). Scale bar, 100 µm. Data represent mean ± SEM. One-way ANOVA with Dunnett's multiple comparisons test, ****p < 0.0001, ***p < 0.001, **p < 0.01, *p < 0.05.

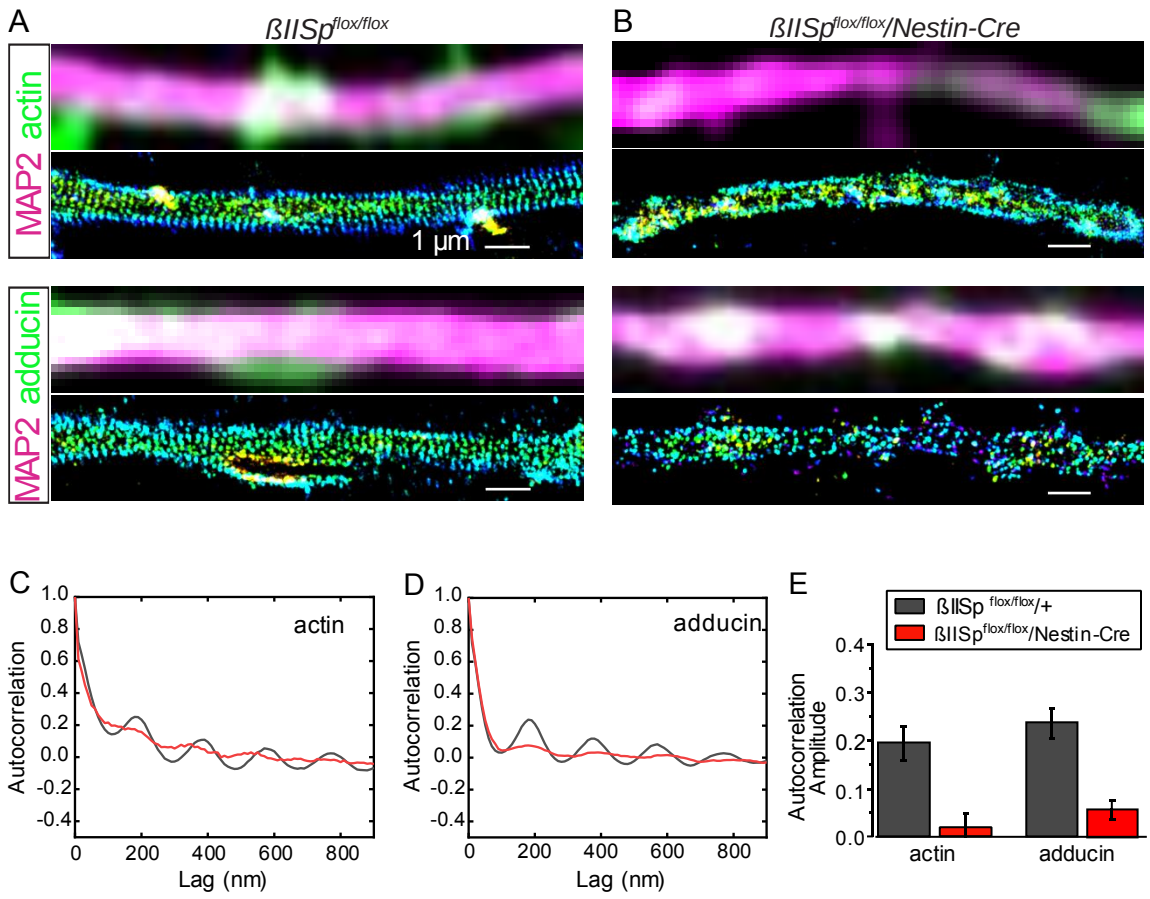

Fig. S7. βII-spectrin is important for the assembly of an actin-spectrin based membrane periodic skeleton structure in dendrites.
(A, B) 3D STORM images of actin (A) and adducin (B) in dendrites of DIV21 control and ßII-SpKO neurons. Scale bar, 1 µm. (C, D) Average autocorrelation functions of actin (C) and adducin (D) calculated from multiple, randomly selected dendritic regions. Actin: (n=53) for *ßIISp*$^{flox/flox}$/+ samples and (n=31) for *ßIISp*$^{flox/flox}$ /Nestin-Cre samples. Adducin: (n=71) for *ßIISp*$^{flox/flox}$/+ samples and n=48 for *ßIISp*$^{flox/flox}$*/Nestin-Cre* samples. (E) Average autocorrelation amplitudes corresponding to actin (C) and adducin (D) periodicity functions in axons. Data represent mean ± SEM.

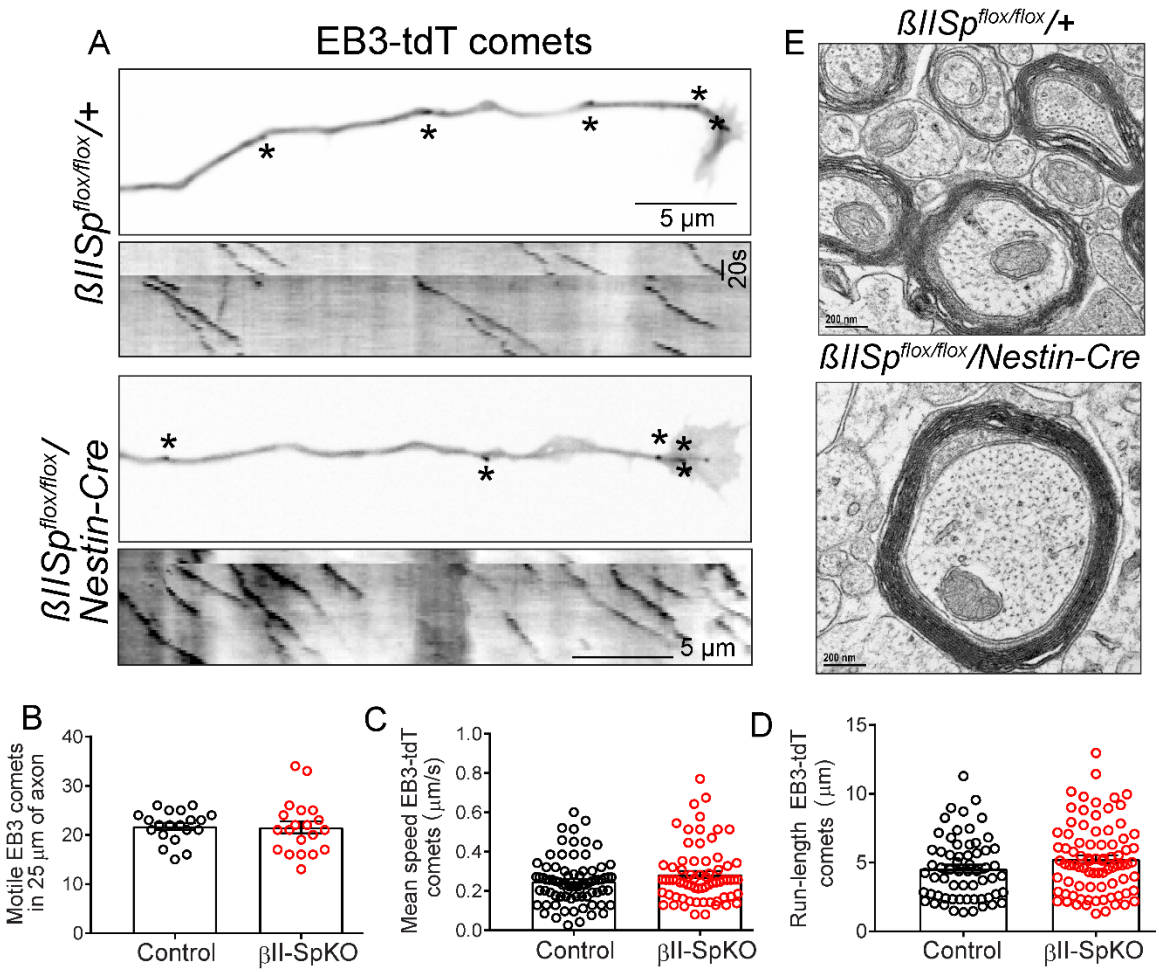

Fig. S8. Loss of neuronal βII-spectrin does not affect axonal microtubule dynamics in cultured neurons and organization of microtubules in non-degenerating axons

(A)Top: Images of DIV5 control and ßII-SpKO neurons expressing EB3-tdT. Scale bar, 5 µm. Asterisks indicate motile EB3-tdT particles. Bottom: Kymographs of EB3-tdT dynamics in axons. Scale bar, 5 µm and 20 s. (B) Number of motile EB3 comets in control and ßII-SpKO axons (n=10). (C) Mean speed of control (n=78) and ßII-SpKO (n=69) EB3 comets in axons. (D) Run-length of control (n=62) and ßII-SpKO (n=82) EB3 comets in axons. Data represent mean ± SEM. Student's t test. (E) TEM images of brain cross sections through the CC from control and ßII-SpKO PND25. Scale bar, 20 nm.

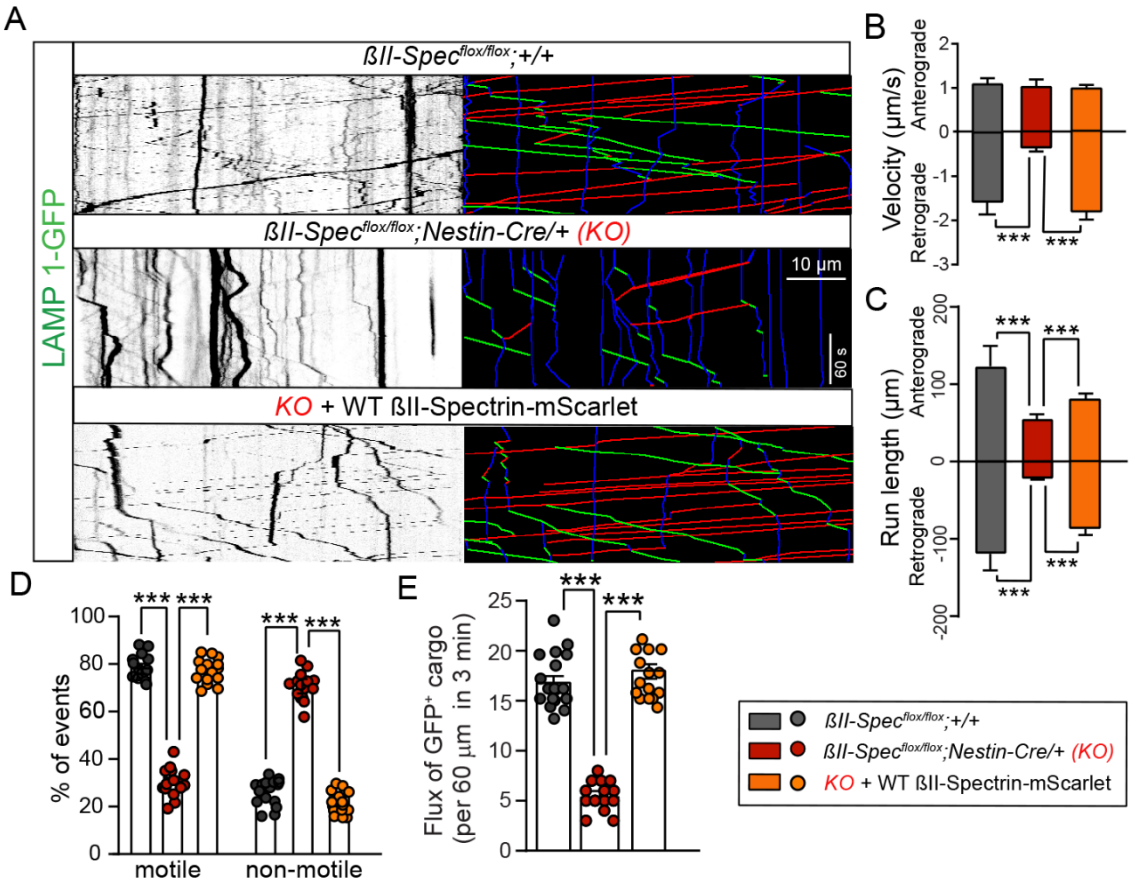

Fig. S9. Loss of βII-spectrin impairs the bidirectional transport of LAMP1-GFP-positive endosomes/lysosomes in axons

(A) Kymographs showing the mobility of GFP-tagged LAMP1-positive cargo in axons from DIV9 control, ßII-SpKO, and rescued ßII-SpKO hippocampal neurons. Trajectories are shown with a color code with green for anterograde, red for retrograde, and blue for static vesicles. Scale bar, 10 µm and 60 s. (B) Anterograde and retrograde velocity *ßIISp*$^{flox/flox}$ (anterograde n=18, retrograde n=24), *ßIISp*$^{flox/flox}$/Nestin-Cre (anterograde n=12, retrograde n=16) axons, and *ßIISp*$^{flox/flox}$/Nestin-Cre neurons transfected with mScarlet-WT βII-spectrin (anterograde n=38, retrograde n=13). (C) and run length of LAMP1-GFP particles. *ßIISp*$^{flox/flox}$ (anterograde n=17, retrograde n=19), *ßIISp*$^{flox/flox}$/Nestin-Cre (anterograde n=18, retrograde n=24) axons, and in axons of *ßIISp*$^{flox/flox}$/Nestin-Cre neurons transfected with mScarlet-WT βII-spectrin (anterograde n=23, retrograde n=21). (D, E) Relative number of motile LAMP1-GFP particles (D) and quantification of flux (E) for each genotype and rescue in *ßIISp*$^{flox/flox}$/+ (n=15), *ßIISp*$^{flox/flox}$/Nestin-Cre (KO) (n=17), KO + WT βII-mScarlet. (n=12) axons of DIV9 hippocampal neurons. Data represent

mean ± SEM. One-way ANOVA with Dunnett's multiple comparisons test, ****p < 0.0001, ***p < 0.001, **p < 0.01, *p < 0.05.

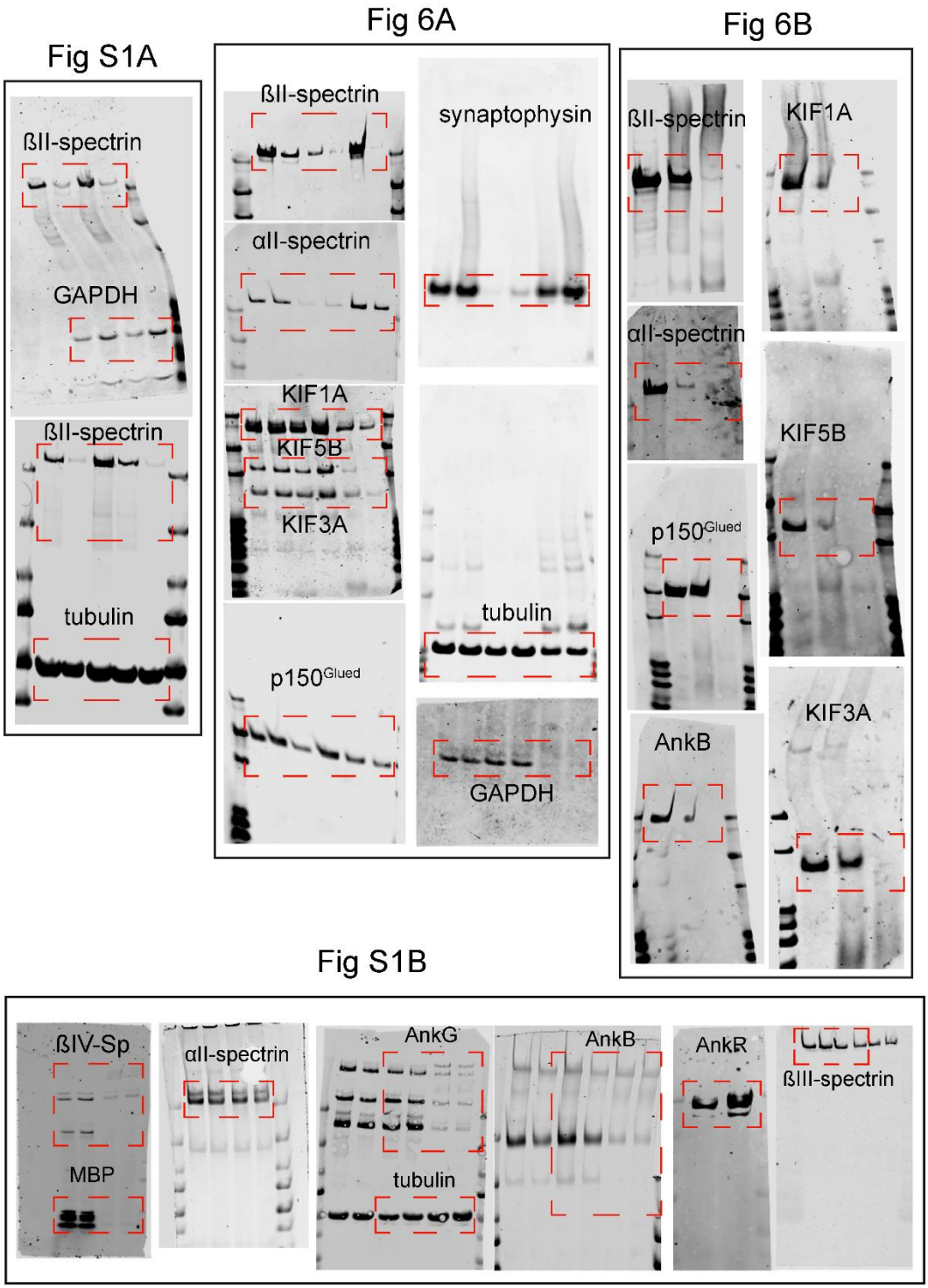

Fig. S10. Original images of Western blots. Red boxes indicate the portion of the images used in the figures.

References

51. Smith SA, et al. (2015) Dysfunction in the βII spectrin-dependent cytoskeleton underlies human arrhythmia. Circulation 131(8):695-708.
52. He M, Abdi KM, Bennett V. (2014) Ankyrin-G palmitoylation and βII-spectrin binding to phosphoinositide lipids drive lateral membrane assembly. *J Cell Biol* 206(2):273-288.
53. Jenkins PM, et al. (2015) Giant ankyrin-G: a critical innovation in vertebrate evolution of fast and integrated neuronal signaling. *Proc Natl Acad Sci USA* 112(4):957-964.
54. Wang S, Cho YK. (2016) An optimized calcium-phosphate transfection method for characterizing genetically encoded tools in primary neurons. *Methods Mol Biol* 1408:243-249.
55. Yeh TY, Quintyne NJ, Scipioni BR, Eckley DM, Schroer TA. (2012) Dynactin's pointed-end complex is a cargo-targeting module. *Mol Biol Cell* 23(19):3827-3837.
56. Huang B, Wang W, Bates M, Zhuang X. (2008) Three-dimensional super-resolution imaging by stochastic optical reconstruction microscopy. *Science* 319:810-813.
57. Zala D, et al. (2013) Vesicular glycolysis provides on-board energy for fast axonal transport. Cell 152(3):479-491.
58. Lustig M, Donoho D, Pauly JM. (2007) Sparse MRI: The application of compressed sensing for rapid MR imaging. *Magn Reson Med* 58(6):1182-1195.
59. Badea A, Gewalt S, Avants BB, Cook JJ, Johnson GA. (2012) Quantitative mouse brain phenotyping based on single and multispectral MR protocols. *Neuroimage* 63(3):1633-1645.
60. Yeh FC, Verstynen TD, Wang Y, Fernández-Miranda JC, Tseng WY. (2013) Deterministic diffusion fiber tracking improved by quantitative anisotropy. *PLoS One* 8(11): e80713.